



ORIGINAL ARTICLE

Diagnostic efficacy of whole-body diffusion-weighted imaging in the detection of tumour recurrence and metastasis by comparison with ¹⁸F-2-fluoro-2-deoxy-D-glucose positron emission tomography or computed tomography in patients with gastrointestinal cancer

Jiaying Gong¹, Wuteng Cao¹, Zhanwen Zhang², Yanhong Deng³, Liang Kang⁴, Pan Zhu¹, Zhengjun Liu¹ and Zhiyang Zhou^{1,*}

¹Department of Radiology, The Sixth Affiliated Hospital (The Gastrointestinal & Anal Hospital) of Sun Yat-sen University, Guangzhou, China, ²Department of Nuclear Medicine, The Sixth Affiliated Hospital (The Gastrointestinal & Anal Hospital) of Sun Yat-sen University, Guangzhou, China, ³Department of Oncology, The Sixth Affiliated Hospital (The Gastrointestinal & Anal Hospital) of Sun Yat-sen University, Guangzhou, China and ⁴Department of Colorectal Surgery, The Sixth Affiliated Hospital (The Gastrointestinal & Anal Hospital) of Sun Yat-sen University, Guangzhou, China

*Corresponding author. Department of Radiology, The Sixth Affiliated Hospital of Sun Yat-sen University, 26 Yuanchun Er Heng Road, Guangzhou, Guangdong 510655, China. Tel: +86-20-38285663; Fax: +86-20-38254054; Email: zhouzyang@hotmail.com

Abstract

Objective: The primary aim of this study was to assess the efficacy of whole-body diffusion-weighted imaging (WB-DWI) in detecting tumour recurrence and metastasis of gastrointestinal cancers by comparison with ¹⁸F-2-fluoro-2-deoxy-D-glucose positron emission tomography or computed tomography (¹⁸F-FDG-PET/CT). A secondary aim was to evaluate the change of apparent diffusion coefficient (ADC) value between metastases and normal tissues.

Methods: Twenty-eight previously confirmed gastrointestinal cancer patients with suspected tumour recurrence or metastasis were recruited. WB-DWI and PET/CT images were evaluated by two radiologists and a nuclear medicine physician. Agreement between WB-DWI and PET/CT for detective efficacy was compared using kappa statistics. Additionally, diagnostic accuracy, sensitivity, specificity, negative predictive value (NPV), and positive predictive value (PPV) were also statistically analysed. ADC values between metastatic and normal tissues were compared.

Results: There was no statistically significant difference ($P > 0.05$) in the overall diagnostic performances of PET/CT (accuracy 98.9%; sensitivity 95.2%; specificity 99.8%; PPV 98.9%; NPV 98.9%) and WB-DWI (accuracy 95.9%; sensitivity 81.7%; specificity 99.1%; PPV 95.0%; NPV 96.1%). WB-DWI showed agreement with PET/CT ($\kappa = 0.877$) for detecting recurrence and distant metastases. A statistically significant difference in ADC value was observed between tissues of normal healthy volunteers and metastases in lymph nodes, liver and bones ($P < 0.05$).

Conclusions: WB-DWI is reliable in detecting tumour recurrence and metastasis of colorectal cancer and offers the same diagnostic performance as ^{18}F -PET/CT without ionizing radiation. The quantitative value of ADC provides extra information to determine cancer metastasis.

Key words: whole-body diffusion-weighted imaging (WB-DWI); ^{18}F -FDG-PET/CT; apparent diffusion coefficient (ADC); colorectal cancer; recurrence; metastasis

Introduction

Gastrointestinal tumour is one of the most common malignant tumours in the world. Oesophageal, stomach and colorectal cancers are leading causes of death worldwide, accounting for 1.8 million deaths (38.9% of all cancer-related deaths) in 2012 [1]. Approximately 40% of patients treated with the most appropriate approach will progress within the first 3 years [2, 3]; however, both recurrence and metastasis from gastrointestinal cancer can be alleviated by curative-intent surgery or intervention [4]. Therefore, early diagnosis and accurate staging of recurrent and metastatic gastrointestinal cancer are important for treatment and prognosis. Multi-modality imaging approaches, including ultrasonography, computed tomography (CT), magnetic resonance imaging (MRI), and ^{18}F -2-fluoro-2-deoxy-D-glucose (FDG) positron emission tomography or computed tomography (PET/CT), have shown promise in diagnosis, staging, monitoring response to therapy and in detecting recurrence and metastasis.

PET/CT has become the most reliable and best-established imaging modality for diagnosis, staging and follow-up of cancers. It also offers prognostic information based on tumours' responses to treatments [5, 6]; however, major disadvantages of PET/CT include exposure of patients to ionizing radiation, the requirement for a cyclotron, and diagnostic interference caused by respiratory artifacts and variable physiological uptake.

Recently, with the development of new MRI scanner and coil technology, whole-body diffusion-weighted imaging (WB-DWI) with background body signal suppression, introduced by Takahara et al. [7], has been recognized as a new imaging modality for the assessment of metastases of various malignancies without radiation exposure and motion artifact [8–10]. Three-dimensional (3D) images can be obtained, using reformatting techniques such as maximum-intensity projection (MIP) and multi-planar reformatted (MPR).

The apparent diffusion coefficient (ADC) map obtained from DWI shows the freedom of water diffusion and values calculated on the map reflect tumour morphology, cellular density, integrity of cell membrane, and nuclear-to-cytoplasm ratio, regardless of the tumour type and location [11, 12]. Limited direct comparison studies have been published on the difference in efficacy between WB-DWI on 1.5T MRI systems and integrated PET/CT, for gastrointestinal cancer staging.

The purpose of this study was to compare the diagnostic performance of WB-DWI with a PET/CT-based standard of reference, in staging previously confirmed gastrointestinal cancer patients with suspected tumour recurrence or metastasis. The second aim was to assess the difference in ADC value between metastatic and normal tissues.

Patients and methods

Patients

Seventy-five patients underwent WB-DWI for staging gastrointestinal cancers with suspected recurrence and metastasis

(including both initial and post-operative cases) in our hospital from October 2012 to November 2013. Among them, 28 patients—20 males and 8 females of ages ranging from 20–78 years (mean age 50 years)—were recruited for the current retrospective study. The inclusion criteria included (i) histopathological confirmation of stomach/oesophageal/colorectal cancer (by gastroscopical/endoscopic biopsy), (ii) simultaneous WB-DWI examination with a PET/CT-based reference for comparison, and/or (iii) clinical/image follow-up of 3–6 months for final judgement. Forty-seven patients were excluded because of histopathological diagnosis of inflammation ($n=5$) and lack of corresponding PET/CT data ($n=42$). Eighteen healthy volunteers were recruited to perform WB-DWI examinations. Written informed consent was obtained from all volunteers.

Primary tumours, confirmed histopathologically in all patients, included oesophageal cancer [initial diagnosis ($n=1$), post-operative follow-up ($n=1$)] in 2 patients (7.1%), gastric cancer [initial diagnosis ($n=1$), post-operative follow-up ($n=2$)] in 3 patients (10.7%), and colorectal cancer [initial diagnosis ($n=9$), and post-operative follow-up ($n=14$)] in 23 patients (82.1%). WB-DWI and PET/CT were performed in these patients within 3–14 days, and none of them received specific therapy (chemotherapy, radiotherapy or surgery) during the interval for study.

Imaging protocols

WB-DWI

MRI examinations were performed on a 1.5T fibre magnetic resonance scanner (GE Optimal 360, USA). The patients were in a supine position and head-first with a body coil. The protocol included short T1 inversion recovery echo-planar imaging diffusion weighted sequence (TR/TE = 4720/87.5 ms) with a diffusion factor (b) of 600 s/mm² and covering the entire body, from the top of the head to the knee. The acquisition was done in an axial plane by segments with fat saturation and inversion recovery pulse (180 ms) to avoid ghosting artifacts due to fat. A slice thickness of 7 mm with no gap and a field of view of 400 mm—as well as 7–8 segments of 30 slices—were necessary, depending on the patient's height. Summation of segments (Sorted Technique) allows whole-body exploration in all planes. Final 'PET-like' images were obtained by coronal reconstruction, using the technique of maximum intensity projection (MIP) and inverted greyscale (Figure 1). The total duration of each examination was about 21 minutes and 30 seconds.

PET/CT

Patients fasted for 6 hours before the examination to ensure blood glucose levels below 150 mg/dL. Furosemide 20 mg was given to increase renal excretion of the tracer and avoid accumulation in non-malignant cells. Examinations were performed 1 hour after an intravenous injection of 5.18 MBq/kg of [^{18}F]-FDG using a hybrid FDG-PET/CT device (Biograph 40 TruePoint with TrueV, Siemens Medical Solutions, Erlangen, Germany) consisting of a high-resolution 3D PET and a 40-row CT. Patients were in a supine position with arms along the body

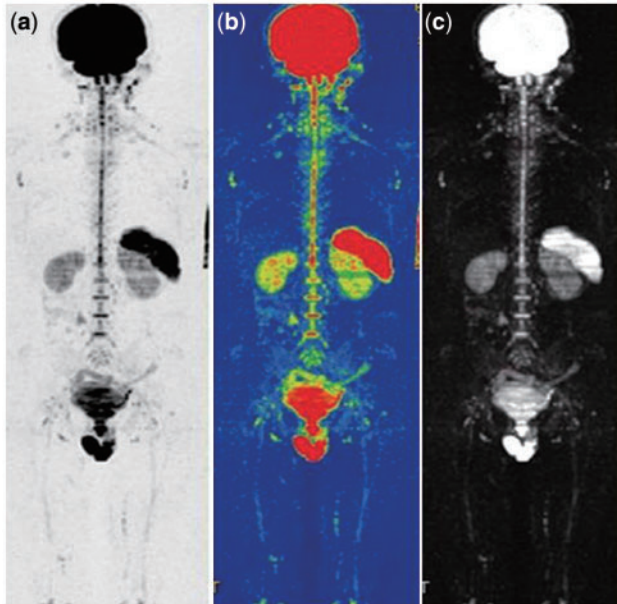


Figure 1. Lungs, mediastinum, liver, pancreas and soft tissue display low signal, while brain, spleen, kidney, bladder, prostate, and testicles show high signal on WB-DWI. (a) Inverted-gray-scale whole-body DWI. (b) Whole-body ADC. (c) Whole-body DWI 3D MIP.

and a field of view from the head to the feet. A whole-body, free-breathing, spiral, low-dose CT acquisition (60 mAs; 120 kV; collimation 2 mm × 5 mm; pitch 1.5) was performed for PET-attenuation correction, followed by the emission scan using a 3D-row action maximum likelihood algorithm (RAMLA) for reconstruction (6–7 bed positions; field of view (FOV) 50 cm; 128 × 128 matrix). A diagnostic contrast-enhanced CT was conducted (100 mAs, 120 kV, collimation 2 × 5 mm, pitch 1) after i.v. administration of 80–90 mL of non-ionic iodinated contrast agent (Iopamiro 300, Bracco, Shanghai, China) in the venous phase (60–70 seconds delay). Finally, PET images were fused with contrast-enhanced CT. The total duration of each examination was about 45 minutes.

Imaging analysis

MRIs were analysed by two board-certified radiologists with more than 8 years of experience in abdominal image and PET/CTs were interpreted by a nuclear medicine physician with 3 years of experience in PET. Both reading groups were fully blinded to the other modality and had no information on previous or current diagnostic imaging results.

Established regions specific for assessing lymph node involvement included the neck, axilla, infra- and supraclavicular region, mediastinum, *hilus pulmonis*, abdominal cavity, retroperitoneum, pelvic cavity, and inguinal region. The most widely accepted criterion for lymph-node involvement, a short diameter of lymph-node greater than 8–10 mm was applied to determine tumour involvement when assessing lymph nodes [13–16]. Solid organ metastases were counted in five body regions including the brain, lungs, liver, adrenal gland, and peritoneum. For diffuse metastatic infiltration patterns, especially in the bones, an evaluation system according to the anatomical regions (skull, scapula, sternum and clavicles, ribs, cervical, thoracic, lumbar and sacral coccygeal vertebrae, pelvis, and extremities) was applied. The number of bone metastases was

assessed in anatomical segments (e.g. diffuse infiltration of one scapula = 1; diffuse infiltration of both clavicles = 2). In the cases of disseminated metastatic disease (defined as more than five countable metastases) in the liver or lungs, the degree of metastatic spread was also described by number of the affected lung lobes and liver segments, respectively (e.g. disseminated metastatic disease in all lung lobes = 5; in all liver segments = 8) [17].

Assessment of lymph nodes, distant metastases and local recurrence on PET/CT images was based on qualitative and quantitative criteria, according to the evidence of regions of focally increased glucose metabolism uptake and maximal standardized uptake value (SUV >2.5 as a reference) [18]. An increased glucose uptake area over the surrounding tissue was considered positive for malignancy.

The WB-DWI original images were processed on a designated workstation (AW4.5, Functool DWI, the company of GE, New York, USA) to produce a unified axial series covering the distance from head to knee, consisting of diffusion-weighted images with diffusion factor (b) = 600 s/mm², and greyscale ADC maps. MIPs around the cranio-caudal axis and MPRs in the coronal plane were reconstructed from the unified DW axial series with b = 600 s/mm² and displayed in inverted greyscale. Metastatic localization, lymph node involvement or the presence of local recurrence were determined by morphological features, size, and signal intensity on DWI.

For ADC value measurements, regions of interest (ROIs), covering the lymph nodes, metastases and normal tissues, were drawn manually on DW images with b = 600 s/mm². On each slice, the high signal intensity of tumour boundaries was traced, and ROIs were copied to the corresponding ADC maps to measure ADC values.

The two imaging modalities were compared for accuracy and efficacy in assessing the disease, on the basis of a lesion-by-lesion overall analysis.

Standard of reference

In staging gastrointestinal tumour, the morphological and functional results obtained by PET/CT analysis served as the main reference standard for comparison with the morphological and signal intensity information obtained by WB-DWI. The results of follow-up with clinical, radiological and even histological examination within a period of 3–6 months also served as a reference for further judgment on which assessment was correct if a suspicion, such as false-positive or negative result, existed in either of both modalities.

Statistical analysis

Concordance between WB-DWI and PET/CT for detecting tumour recurrence and metastasis was analysed using kappa statistics. The diagnostic accuracy, sensitivity and specificity, as well as positive- and negative predictive values (PPV and NPV) of both modalities, were statistically calculated. Statistical analyses were performed using SPSS for Windows (Version 13.0; SPSS Inc., Chicago, USA). For ADC value analysis, the mean, standard deviation, median and interquartile range were used. Independent-samples *t*-test was used to analyse the variables between metastatic and normal tissues of liver and lymph node. Mann-Whitney *U*-test was used to analyse the variables between metastatic and normal tissues of Vertebrae. Paired-samples *t*-test was used to analyse the difference for overall diagnostic performances between PET/CT and WB-DWI. Crosstabs were used to analyse the concordance between PET/CT and WB-DWI. A *P*-

value of less than 0.05 was considered statistically significant for all tests. Agreement was considered poor when κ was less than 0.40, moderate when $0.75 > \kappa \geq 0.4$, and perfect when $\kappa \geq 0.75$.

Results

WB-DWI examinations were successfully completed in all volunteers without unreadable MRIs due to motion artifacts. One

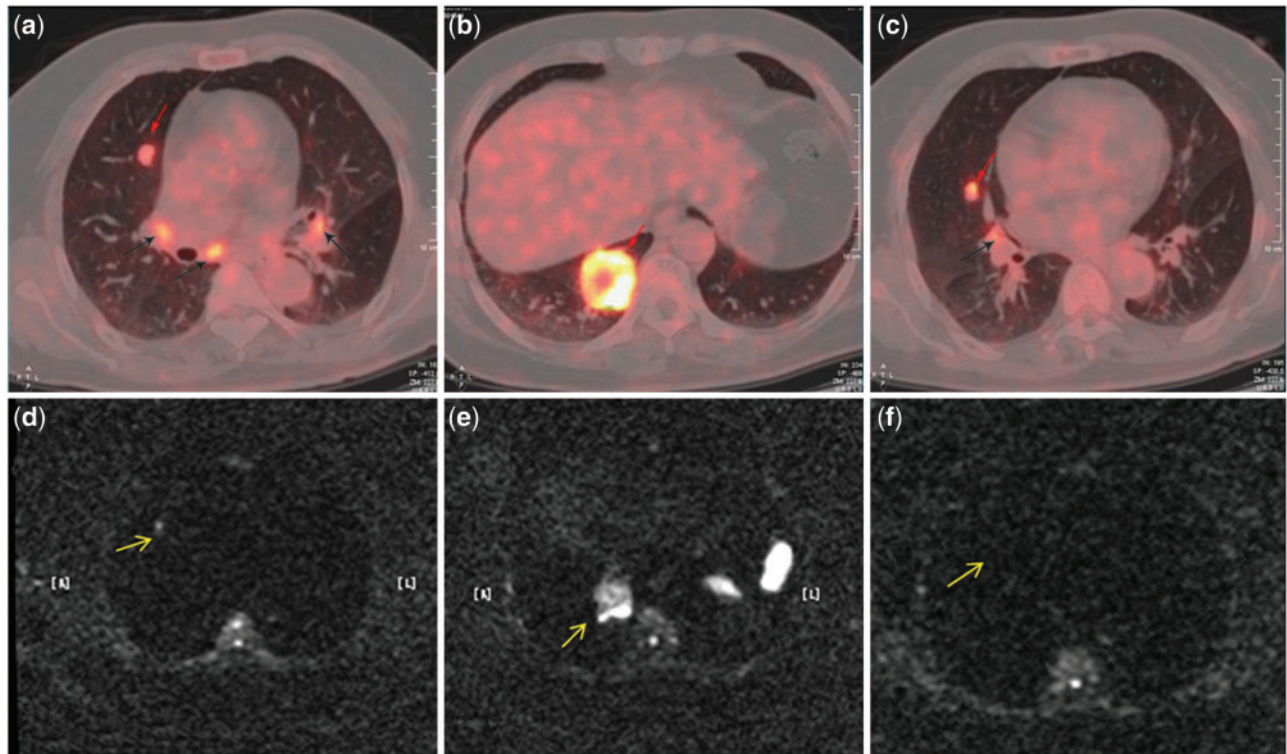


Figure 2. A routine follow-up examination of a 62-year-old woman after rectal cancer surgery. (a, b, c) PET/CT images detected three metastases in the right lung (red arrows) and four metastatic hilar lymph nodes (black arrows). (d, e, f) The corresponding axial WB-DWI ($b = 600 \text{ s/mm}^2$) showed two hyperintense lesions in the right lung (yellow arrow). One nodule in the right middle lobe was missed on WB-DWI (f).

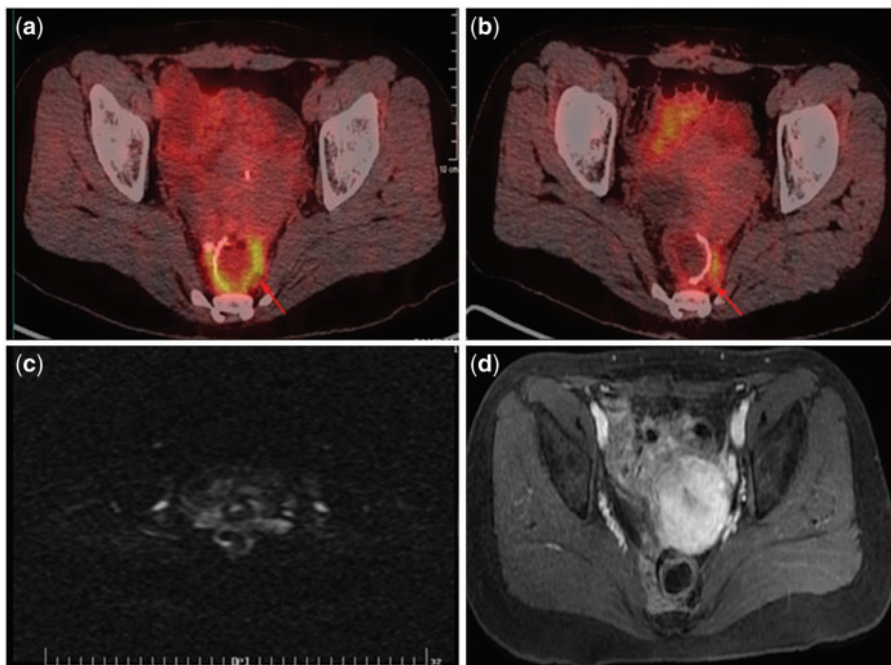


Figure 3. False-positive recurrence on PET/CT of a 38-year-old woman after rectal cancer surgery. (a, b) PET/CT images show increased FDG uptake ($\text{SUV}_{\text{max}} 7.9$) around anastomotic site (red arrows). (c) The corresponding axial WB-DWI image ($b = 600 \text{ s/mm}^2$) shows normal. (d) Follow-up MRI after 3 months demonstrated no recurrence on axial LAVA-flex with i.v. contrast in the pelvic cavity.

patient was considered free of tumour recurrence and metastasis by both WB-DWI and PET/CT. Primary and metastatic lesions were detected and identified as hyperintense on WB-DWI in 26 of the 28 patients (92.9%) (Figure 2). Local tumour recurrences in two patients were detected by PET/CT but denied by WB-DWI (Figure 3), which was considered as false-positive on PET/CT, since no signs of tumour recurrence were found on 3-month

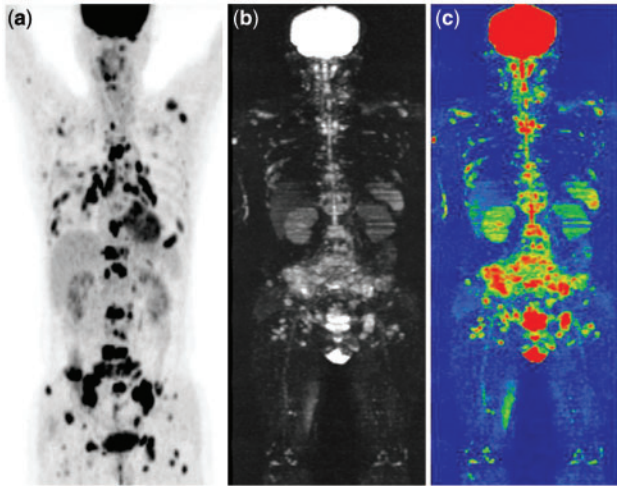


Figure 4. PET/CT (a), WB-DWI (b) and whole-body ADC (c) successfully diagnosed metastases in the sternum, the whole spine, the pelvis, the extremities, and multiple cervical, axillary, mediastinal, pulmo-hilar, abdominal, retroperitoneal, and inguinal lymph nodes in a 51 year-old male after rectal cancer surgery.

MRI follow-up. Thirty-four bone metastases demonstrated as high signal intensity on WB-DWI (Figure 4) were also shown on PET/CT, while another 6 lesions (1 rib, 1 pelvis, 4 vertebrae), missed on WB-DWI, were also shown on PET/CT. One metastatic lesion in the brain, detected by WB-DWI, was missed on PET/CT imaging (Figure 5). PET/CT detected more lymph node metastases than WB-DWI (72 vs. 64). For the detection of distant metastatic disease, PET/CT revealed more lung metastases (21 vs. 10). Alternatively, WB-DWI revealed more metastases of the liver (16 vs. 10) (Table 1).

PET/CT showed an overall diagnostic accuracy of 98.9% (95% CI 97.9–100%) with a sensitivity of 95.2% (95% CI 67.7–95.7%), a specificity of 99.8% (95% CI 99.5–100%), a PPV of 98.9% (95% CI 77.1–100%), and an NPV of 98.9% (95% CI 97.8–100%). WB-DWI achieved an overall diagnostic accuracy of 95.9% (95% CI 93.9–98.2%) with a sensitivity of 81.7% (95% CI 67.7–92.7%), a specificity of 99.1% (95% CI 98.3–100%), a PPV of 95.0% (95% CI 70.5–95.8%) and an NPV of 96.1% (95% CI 92.2–98.5%). An overview of calculated diagnostic performance is provided in Table 2. For overall diagnostic performances, no statistically significant difference (paired-samples $t = 1.332$; $P = 0.194$) was observed between PET/CT and WB-DWI. Meanwhile, WB-DWI showed a good agreement with PET/CT ($\kappa = 0.877$) for detecting recurrence and distant metastases.

The mean ADC value of normal liver, lymph node and vertebrae was $(2.36 \pm 0.27) \times 10^{-3} \text{ mm}^2/\text{s}$, $(2.35 \pm 0.17) \times 10^{-3} \text{ mm}^2/\text{s}$ and $(1.40 \pm 0.44) \times 10^{-3} \text{ mm}^2/\text{s}$, respectively. The mean ADC value of liver, lymph node and vertebral metastases was $(1.59 \pm 0.15) \times 10^{-3} \text{ mm}^2/\text{s}$ (26 ROIs), $(1.31 \pm 2.12) \times 10^{-3} \text{ mm}^2/\text{s}$

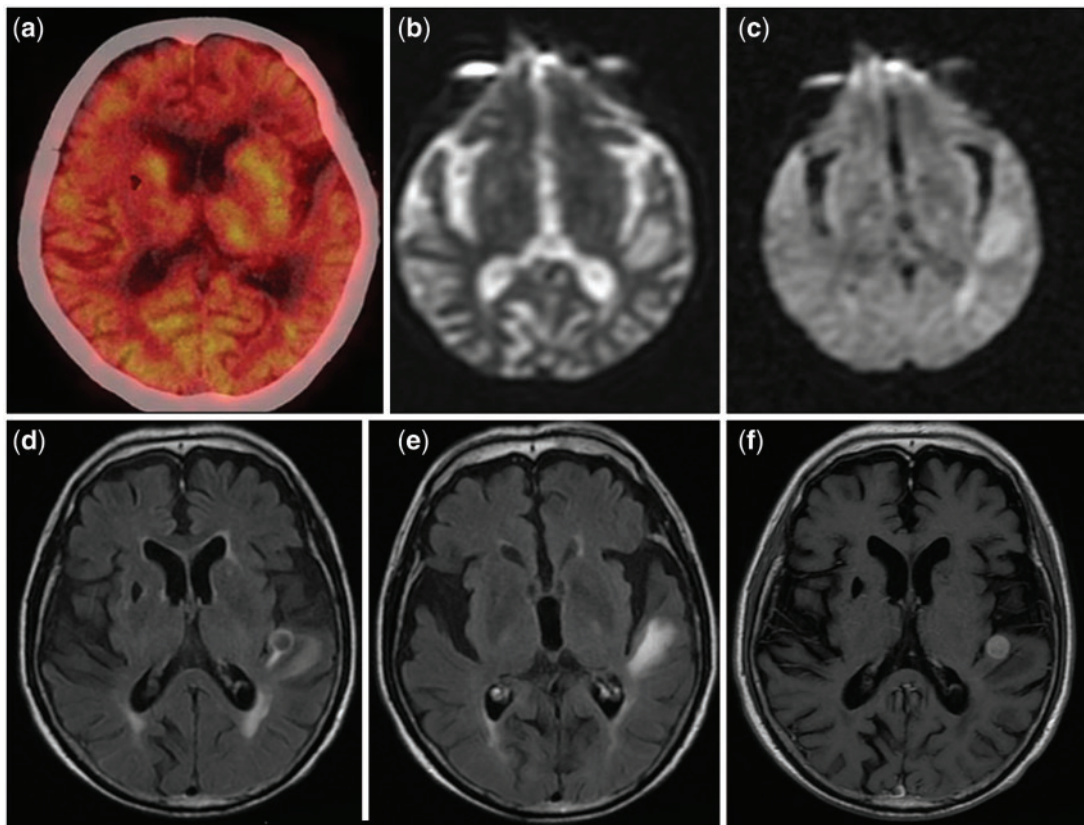


Figure 5. The follow-up examination of an 82-year-old man after rectal cancer surgery showed false-negative PET/CT for brain metastasis (a). The axial WB-DWI images (b: $b = 0 \text{ s}/\text{mm}^2$; c: $b = 600 \text{ s}/\text{mm}^2$) detected hyperintensity in the left temporal lobe. The hyperintensity was confirmed as a typical brain metastatic nodule and edema around the lesion on MRI FLAIR (d, e) and T1WI with i.v. contrast (f). The prior brain CT examination was normal (not shown).

Table 1. Local and metastatic lesions detected by positron emission tomography/computed tomography and whole-body diffusion-weighted imaging scans

Location of lesions	Number of lesions detected	
	PET/CT	WB-DWI
Local primary/recurrent lesions	20	19
Oesophagus	2	2
Stomach	3	3
Colorectum	15	14
Bone metastases	40	34
Skull	1	1
Scapula	1	1
Sternum and clavicles	1	1
Rib	2	1
Vertebrae (cervical, thoracic, lumbar and sacro-coccygeal)	29	25
Pelvis	4	3
Extremity	2	2
Lymph node involvements	72	64
Cervical	1	0
Axillary	3	2
Infra-or supra-clavicular	5	5
Mediastinal	8	7
Pulmo-hilar	7	5
Abdominal	11	11
Retroperitoneal	18	17
Pelvic	13	10
Inguinal	6	7
Organ metastasis	47	43
Brain	0	1
Lung	21	10
Liver	10	16
Adrenal gland	2	2
Peritoneum	14	14
Total	179	160

PET/CT = positron emission tomography/computed tomography; WB-DWI = whole-body diffusion-weighted imaging

(23 ROIs) and $(0.95 \pm 0.30) \times 10^{-3} \text{ mm}^2/\text{s}$ (21 ROIs), respectively. There was a statistically significant difference in ADC values between normal liver, lymph nodes and vertebrae in healthy volunteers and corresponding metastases in gastrointestinal tumour patients (all $P < 0.001$; Table 3).

Discussion

Despite the high prevalence of recurrent and metastatic disease among patients suffering from gastrointestinal cancer, both local recurrence and limited metastatic disease can be successfully managed by curative-intent surgery or neoadjuvant intervention, with significantly improved survival rates [19–21]. Early diagnosis and accurate staging of lesions are therefore important in defining appropriate therapeutic strategies.

PET-CT has become the established, standard imaging modality for cancer staging and evaluation of response to treatment, because it provides both anatomical and functional information [22, 23]. WB-DWI is very successful in detecting cancers. In a study of 33 cases, Ichikawa *et al.* examined the feasibility of diffusion-weighted imaging with background body signal suppression (DWIBS) in detecting colorectal cancers and evaluated the primary lesions, reporting 91% for sensitivity and 100% for specificity [24]. Several other studies have described PET/CT as an effective imaging strategy for the staging of

Table 2. Diagnostic efficacy of positron emission tomography/computed tomography and whole-body diffusion-weighted imaging scans in detecting recurrent and metastatic lesions

Diagnostic efficacy	PET/CT	WB-DWI
True positive (n)	177	152
False-positive (n)	2	8
True negative (n)	848	842
False-negative (n)	9	34
Accuracy % (95% CI)	98.9 (97.9–100)	95.9 (93.9–98.2)
Sensitivity % (95% CI)	95.2 (67.7–95.7)	81.7 (67.7–92.7)
Specificity % (95% CI)	99.8 (99.5–100)	99.1 (98.3–100)
Positive predictive value % (95% CI)	98.9 (77.1–100)	95.0 (70.5–95.8)
Negative predictive value % (95% CI)	98.9 (97.8–100)	96.1 (92.2–98.5)

PET/CT = positron emission tomography/computed tomography; WB-DWI = whole-body diffusion-weighted imaging

Table 3. Comparison of apparent diffusion coefficient (ADC) value between normal tissues of volunteers and metastases of patients

Location	ADC value ($\times 10^{-3} \text{ mm}^2/\text{s}$)		t/Z	P-value
	Normal	Metastatic		
Liver	2.36 ± 0.27	1.59 ± 0.15	12.08 (t)	<0.001
Lymph node	2.35 ± 0.17	1.31 ± 0.12	18.20 (t)	<0.001
Vertebrae	1.40 ± 0.44	0.95 ± 0.30	-5.171 (Z)	<0.001

colorectal cancer, with a reported sensitivity of 89–98% and specificity of 83–96% [25–27]. In our study, no statistically significant difference was seen between the two imaging modalities in detecting metastases ($P < 0.001$) (PET/CT with an overall diagnostic accuracy of 98.9% and specificity of 99.8% vs. WB-DWI with an overall diagnostic accuracy of 95.9%, and specificity of 99.1%).

Two patients in whom there was a false-positive finding of tumour recurrence by PET/CT at the rectal anastomosis showed no signs of recurrence by WB-DWI and follow-up MRI examinations. Increased FDG uptake in inflammatory disease and inadequate bowel distension may mimic a suspicious mass with circumscribed tracer accumulation, as demonstrated in these two patients (Figure 3). In the case of ambiguous findings, a close follow-up examination is advised and sometimes endoscopic colonoscopy with lesion biopsy may be needed if results remain inconclusive.

In our study, we observed a higher diagnostic sensitivity of 95.2% for PET/CT than the figure of 81.7% for WB-DWI. This discrepancy may be primarily due to the higher sensitivity for PET/CT in detecting lung metastases (21 vs. 10). It has been reported that WB-DWI is unable to detect lung lesions less than 6 mm in diameter, which results in false-negative findings [28]. Therefore, improvements are still needed before WB-DWI can be used as an alternative to CT in routine clinical assessment of the lungs. Although low-dose thoracic CT acquisition in the inspiratory phase in PET/CT protocols may improve sensitivity for lesions smaller than 8 mm, the clinical relevance of such modified protocols remains unclear [29]. Thus, the best ways of detecting small lung metastases may differ according to the specific clinical settings.

Evaluating the metastatic lymph nodes in cancer patients with DWI is challenging. With the development of MRI sequences, the lymph nodes can be made clearly visible in the suppressed background tissues on DWI, but most studies have

shown that DWI falls short in separating benign from malignant lymph nodes according to their hyperintensity, because normal lymph nodes already have a relatively long T2 relaxation time and a restricted diffusion, due to their high cellularity [30]. In our study, PET/CT was better in detecting lymph node metastasis than WB-DWI (72 vs. 64), especially in the typical regions of lymphogenic metastatic dissemination from rectal and oesophageal cancer, such as in the pelvic cavity, mediastinum, *hilus pulmonis*, and regions along the iliac artery and thoracic aorta, where image quality may be affected by pulsation or susceptibility artifacts on MRI.

It has been commonly believed that PET/CT is inferior to WB-DWI in detecting metastasis in the liver and brain, due to the high physiological tracer uptake in these organs [31, 32]. In our study, we detected 16 hepatic metastases by WB-DWI and only 10 by PET/CT. One metastatic lesion in the left temporal lobe of the brain was missed by PET/CT (Figure 5).

WB-DWI is a reliable technique in evaluating bone metastasis, with detailed anatomical information on the axial and appendicular skeleton [33, 34]. Our results demonstrated a lower diagnostic performance for WB-DWI than for PET/CT. The six additional lesions detected by PET/CT and ignored by WB-DWI were small metastases in vertebrae and ribs, where additional motion artifacts of respiration and pulsation impaired image quality.

A statistically significant difference in ADC values was observed between metastases in various regions (including liver, lymph nodes in retroperitoneal space and pelvic cavity, thoracolumbar vertebrae, etc.) and corresponding normal tissues in healthy volunteers; however, this result reflects only higher cellularity or proliferation in the lesions, which is still insufficient for evaluating their specificity. In some studies, authors have reported that ADC values are also inadequate for differentiating malignant from benign lymph nodes [35]. Thus, its clinical application is still under investigation [36].

In conclusion, both PET/CT and WB-DWI demonstrate an excellent diagnostic accuracy in detecting tumour recurrence and metastases of gastrointestinal cancer. DWIBS is superior to PET/CT in terms of lower price, lack of ionizing radiation, higher spatial resolution, and better assessment for non-FDG-avid tumour types and organs with high lesion-to-background contrast. WB-DWI may in the foreseeable future become a reliable alternative modality for staging cancer patients.

Acknowledgements

The authors would like to thank Prof Kunhao Fang and Ting Wang for their contributions on English correction to this study. In addition, we thank Yanbang Lian for his help in the statistical analysis.

Conflict of interest statement: none declared.

References

- World Health Organization. Globocan 2012: Estimated Cancer Incidence, Mortality and Prevalence Worldwide in 2012. http://globocan.iarc.fr/Pages/fact_sheets_cancer.aspx.
- Desch CE, Benson AR, Somerfield MR et al. Colorectal cancer surveillance: 2005 update of an American Society of Clinical Oncology practice guideline. *J Clin Oncol* 2005;23:8512–19.
- Abir F, Alva S, Longo WE et al. The postoperative surveillance of patients with colon cancer and rectal cancer. *Am J Surg* 2006;192:100–8.
- Gillams AR and Lees WR. Five-year survival following radio-frequency ablation of small, solitary, hepatic colorectal metastases. *J Vasc Interv Radiol* 2008;19:712–17.
- Soydal C, Yuksel C, Kucuk NO et al. Prognostic Value of Metabolic Tumor Volume Measured by 18F-FDG PET/CT in Esophageal Cancer Patients. *Mol Imaging Radionucl Ther* 2014; 23:12–15.
- von Schulthess GK, Steinert HC and Hany TF. Integrated PET/CT: current applications and future directions. *Radiology* 2006; 238:405–22.
- Takahara T, Imai Y, Yamashita T et al. Diffusion weighted whole body imaging with background body signal suppression (DWIBS): technical improvement using free breathing, STIR and high resolution 3D display. *Radiat Med* 2004;22: 275–82.
- Akay S, Kocaoglu M, Emer O et al. Diagnostic accuracy of whole-body diffusion-weighted magnetic resonance imaging with 3.0 T in detection of primary and metastatic neoplasms. *J Med Imaging Radiat Oncol* 2013;57:274–82.
- Sakurai Y, Kawai H, Iwano S et al. Supplemental value of diffusion-weighted whole-body imaging with background body signal suppression (DWIBS) technique to whole-body magnetic resonance imaging in detection of bone metastases from thyroid cancer. *J Med Imaging Radiat Oncol* 2013;57: 297–305.
- Wang N, Zhang M, Sun T et al. A comparative study: diffusion weighted whole body imaging with background body signal suppression and hybrid Positron Emission Computed Tomography on detecting lesions in oncologic clinics. *Eur J Radiol* 2012;81:1662–66.
- Castillo M, Smith JK, Kwock L et al. Apparent diffusion coefficients in the evaluation of high-grade cerebral gliomas. *AJNR Am J Neuroradiol* 2001;22:60–64.
- Nonomura Y, Yasumoto M, Yoshimura R et al. Relationship between bone marrow cellularity and apparent diffusion coefficient. *J Magn Reson Imaging* 2001;13:757–60.
- Glazer GM, Gross BH, Quint LE et al. Normal mediastinal lymph nodes: number and size according to American Thoracic Society mapping. *AJR Am J Roentgenol* 1985;144: 261–65.
- Dorfman RE, Alpern MB, Gross BH et al. Upper abdominal lymph nodes: criteria for normal size determined with CT. *Radiology* 1991;180:319–22.
- Som PM, Curtin HD and Mancuso AA. Imaging-based nodal classification for evaluation of neck metastatic adenopathy. *AJR Am J Roentgenol* 2000;174:837–44.
- Suzuma T, Sakurai T, Yoshimura G et al. A mathematical model of axillary lymph node involvement considering lymph node size in patients with breast cancer. *Breast Cancer* 2001;8:206–12.
- Schmidt GP, Baur-Melnyk A, Haug A et al. Comprehensive imaging of tumor recurrence in breast cancer patients using whole-body MRI at 1.5 and 3 T compared to FDG-PET-CT. *Eur J Radiol* 2008;65:47–58.
- Beggs AD, Hain SF, Curran KM et al. FDG-PET as a “metabolic biopsy” tool in non-lung lesions with indeterminate biopsy. *Eur J Nucl Med Mol Imaging* 2002;29:542–46.
- Arriola E, Navarro M, Pares D et al. Imaging techniques contribute to increased surgical rescue of relapse in the follow-up of colorectal cancer. *Dis Colon Rectum* 2006;49: 478–84.

20. Kemmochi T, Egawa T, Mihara K et al. [Neoadjuvant chemotherapy with capecitabine plus oxaliplatin and bevacizumab for the treatment of patients with resectable metastatic colorectal cancer]. *Gan To Kagaku Ryoho* 2013;**40**:1629–31.
21. Vigano L, Ferrero A, Lo TR et al. Liver surgery for colorectal metastases: results after 10 years of follow-up. Long-term survivors, late recurrences, and prognostic role of morbidity. *Ann Surg Oncol* 2008;**15**:2458–64.
22. Malkowski B, Staniuk T, Srutek E et al. (18)F-FLT PET/CT in Patients with Gastric Carcinoma. *Gastroenterol Res Pract* 2013; **2013**:696423.
23. la Fougere C, Hundt W, Brockel N et al. Value of PET/CT versus PET and CT performed as separate investigations in patients with Hodgkin's disease and non-Hodgkin's lymphoma. *Eur J Nucl Med Mol Imaging* 2006;**33**:1417–25.
24. Ichikawa T, Erturk SM, Motosugi U et al. High-B-value diffusion-weighted MRI in colorectal cancer. *AJR Am J Roentgenol* 2006;**187**:181–84.
25. Even-Sapir E, Parag Y, Lerman H et al. Detection of recurrence in patients with rectal cancer: PET/CT after abdominoperineal or anterior resection. *Radiology* 2004;**232**:815–22.
26. Chen LB, Tong JL, Song HZ et al. (18)F-DG PET/CT in detection of recurrence and metastasis of colorectal cancer. *World J Gastroenterol* 2007;**13**:5025–29.
27. Ma Q, Xin J, Zhao Z et al. Value of (18)F-FDG PET/CT in the diagnosis of primary gastric cancer via stomach distension. *Eur J Radiol* 2013;**82**:e302–e306.
28. Frericks BB, Meyer BC, Martus P et al. MRI of the thorax during whole-body MRI: evaluation of different MR sequences and comparison to thoracic multidetector computed tomography (MDCT). *J Magn Reson Imaging* 2008;**27**:538–45.
29. Juergens KU, Weckesser M, Stegger L et al. Tumor staging using whole-body high-resolution 16-channel PET-CT: does additional low-dose chest CT in inspiration improve the detection of solitary pulmonary nodules? *Eur Radiol* 2006;**16**: 1131–37.
30. Holzapfel K, Duetsch S, Fauser C et al. Value of diffusion-weighted MR imaging in the differentiation between benign and malignant cervical lymph nodes. *Eur J Radiol* 2009;**72**: 381–7.
31. Laurent V, Trausch G, Bruot O et al. Comparative study of two whole-body imaging techniques in the case of melanoma metastases: advantages of multi-contrast MRI examination including a diffusion-weighted sequence in comparison with PET-CT. *Eur J Radiol* 2010;**75**:376–83.
32. Jovet JC, Thomas L, Thomson V et al. Whole-body MRI with diffusion-weighted sequences compared with 18 FDG PET-CT, CT and superficial lymph node ultrasonography in the staging of advanced cutaneous melanoma: a prospective study. *J Eur Acad Dermatol Venereol* 2013;**24**:176–85.
33. Michielsen K, Vergote I, Op de Beeck K et al. Whole-body MRI with diffusion-weighted sequence for staging of patients with suspected ovarian cancer: a clinical feasibility study in comparison to CT and FDG-PET/CT. *Eur Radiol* 2014;**24**:889–901.
34. Barcelo J, Vilanova JC, Riera E et al. [Diffusion-weighted whole-body MRI (virtual PET) in screening for osseous metastases]. *Radiologia* 2007;**49**:407–15.
35. Kwee TC, Takahara T, Luijten PR et al. ADC measurements of lymph nodes: inter- and intra-observer reproducibility study and an overview of the literature. *Eur J Radiol* 2010;**75**:215–20.
36. Murtz P, Krautmacher C, Traber F et al. Diffusion-weighted whole-body MR imaging with background body signal suppression: a feasibility study at 3.0 Tesla. *Eur Radiol* 2007;**17**: 3031–37.